Copyright © 2017 American Scientific Publishers
All rights reserved
Printed in the United States of America

Nanoscience and Nanotechnology Letters
Vol. 9, 1271–1277, 2017

Die Bonding Using Submicrometer Ag-Coated Cu Particles and Enhancement of Bonding Strength by Resin Infiltration

Chang Hyun Lee and Jong-Hyun Lee*

Department of Materials Science and Engineering, Seoul National University of Science and Technology, Seoul 139-743, Republic of Korea

To form a bondline that is suitable for high-power dies, die bonding using submicrometer Ag-coated Cu particles was performed at temperatures above 200 °C. The solid-state Ag dewetting behavior was found to be sensitive to temperature. The formation of bump-like structures on the particle surface and slight bonding between the particles were observed after heating for 20 min at 225 °C. After heating at 250 °C, a rougher surface, strong bonding between the particles, and out-diffusion of Cu through the Ag layer were observed. As a result, the outermost phase was determined to be a Cu_2O phase. The bonding strength of the die increased with increasing bonding temperature and time. Although a die bonded for 20 min at 250 °C without the application of any bonding pressure initially exhibited a strength of 2.250 MPa, the strength increased to 19.991 MPa with increased displacement as a result of resin infiltration and curing. This paper is the first report on the feasibility of die bonding using *in situ* dewetting behavior with submicrometer Ag-coated Cu particles.

Keywords: Die Bonding, Silver-Coated Copper, Nanoscale Silver Dewetting, Resin Infiltration, Shear Strength.

1. INTRODUCTION

In response to the ongoing demand for inexpensive materials for electronics packaging, extensive studies have been conducted on Ag-coated Cu particles in recent years.[1–17] Given that Cu particles exhibit electrical conductivity similar to Ag, they can be used as a more price-competitive alternative to the Ag filler that has conventionally been the most popular filler material for conductive pastes.[18, 19] An Ag coating also prevents the oxidation of Cu, both at room temperature and when heated in air at temperatures up to 200 °C.[4, 7, 10, 11, 13]

However, some reports have noted that solid-state Ag dewetting occurs in the coating layer when the particles are heated to temperatures more than 200 °C, thus causing the core Cu to oxidize.[9, 14, 15, 20] Hai et al. investigated the thermal oxidation properties of 5-μm Ag-coated Cu particles and observed the Ag dewetting phenomenon on the Cu surface at approximately 200 °C.[9] The formation of an interface between the Ag shell and the Cu core particle in a Ag–Cu binary system increases the instability at the interface and finally induces solid-state dewetting of the Ag shell. Hence, it has been assumed that conductive pastes containing only Ag-coated Cu particles as their filler should not be exposed to temperatures higher than 200 °C.

This study sets out to devise a die-bonding process using the solid-state Ag dewetting phenomenon. Similar research was previously undertaken by Park et al.[21] They prepared Ag particles 30–60 nm in diameter and attached them to Cu flakes. Their results confirmed the occurrence of necking and grain growth between the Ag particles on the Cu flakes after heating at 250 °C without the application of any pressure. The results indicated that there was a connection between the Ag-precipitated Cu flakes and the feasibility of bonding between the flakes. However, the Cu flakes oxidized easily, and so real die bonding using the flakes was not attempted.

In this study, we set out to fabricate Ag bumps on the Cu surface *in situ* by taking advantage of the solid-state Ag dewetting phenomenon in submicrometer Ag-coated Cu particles during heating. The curvature of the submicrometer particles may promote the Ag dewetting behavior owing to the increased surface energy per unit area. Moreover, the thickness of the Ag shell can be limited to within 18 nm. After the thin Ag shell is transformed into small bumps of less than 20 nm diameter, the melting point drops significantly due to the Gibbs–Thomson effect,[22, 23] which

*Author to whom correspondence should be addressed.

greatly facilitates the sintering. The bondline formed by bonding between the Ag-coated Cu particles would be suitable for high-power dies because the bondline would not melt until the temperature reached the eutectic point of Ag and Cu (779 °C).

2. EXPERIMENTAL DETAILS

The Ag-coated Cu particles used in this study were fabricated in-house. They had an average diameter of approximately 860 nm. The fabrication method and detailed characterization of the particles, including the coverage of the Ag shell, were reported in a previous paper.[13] The Ag-coated Cu particles were mixed with α-terpineol (98.5%, Samchun Chemical Co., Ltd.) at a weight ratio of 8:2 to prepare a paste. The paste was printed onto a 10×10 mm Ag-finished Si substrate through a stencil mask with a slit volume of $4 \times 4 \times 0.1$ mm using a squeegee. Finally, a 4×4 mm Ag-finished Si chip was placed on the printed paste.

The die bonding was conducted using the paste for 3, 10, and 20 min at 200, 225, and 250 °C. No pressure was applied during the bonding. After the bonding, infiltration and curing of an epoxy-based resin formulation (ACCP150, Hojeonable, Inc.) through the bondline were also conducted. The formulation was injected to only one side of the bonded die using a syringe, after which the resin was cured for 1 h at 150 °C.

The size, morphology, and microstructure of the particles were analyzed using a field-emission scanning electron microscope (FESEM, JSM-6700F, JEOL Ltd.). To indicate the distribution of the Ag phase in cross-sectional images, back-scattered electron (BES) mode was also applied. The phase change in the Ag-coated Cu particles after heating in air was analyzed by X-ray diffraction (XRD, D8 Advance, Bruker AXS). Finally, the shear strength of the bonded die was measured using a tip speed of 200 μm/s and a tip height of 50 μm using a shear tester (Dage 2000, Precision Industries Ltd.).

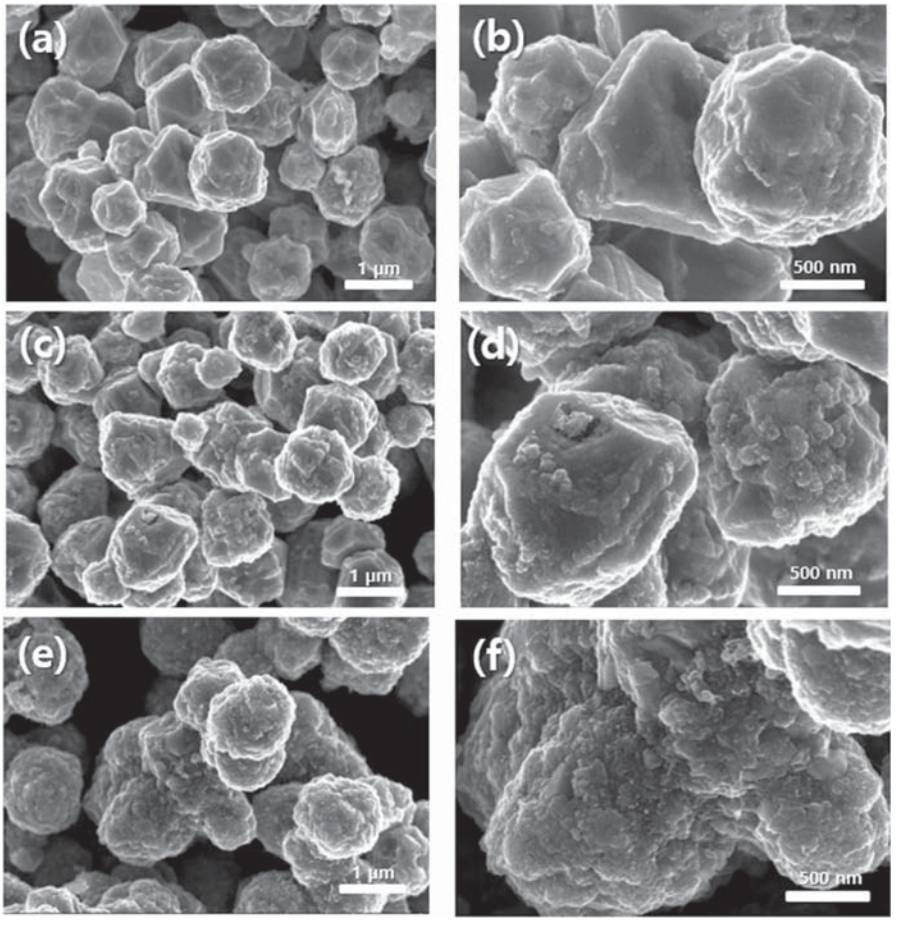

Fig. 1. Low- and high-magnification SEM images of Ag-coated Cu particles after heat treatment for 20 min at different temperatures: (a, b) 200 °C, (c, d), 225 °C, and (e, f) 250 °C.

3. RESULTS AND DISCUSSION

Figure 1 shows SEM images of Ag-coated Cu particles heated for 20 min at different temperatures. When the particles were heated to 200 °C, the morphological changes in the particles were minor. When the particles were heated to 225 °C, however, many surface bumps were clearly observed. Given the initial surface of the Ag-coated Cu particles, we can assume that the bumps were caused by the morphological evolution of the Ag shell. After heating to 250 °C, the surfaces of the particles became rougher, and aggregation between particles was observed to increase. However, we were able to determine that the roughness of the surfaces of the different specimens heated to temperatures of between 225 °C and 250 °C varied slightly.

Figure 2 shows cross-sectional BSE images of the Ag-coated Cu particles heated for 20 min at different temperatures. In the BSE images, the Ag shell appears as a bright color because Ag is heavier than Cu. Although the Ag shell thickness is slightly irregular, it is evident that the Ag shell did not transform into the bumpy shapes seen in the particles heated to 200 °C. On the other hand, many Ag bumps formed on the surfaces of the particles heated to 225 °C, and bonding between the particles was also observed when the particles were in contact. This indicates that the solid-state dewetting behavior of the Ag shell on a Ag-coated Cu particle is sensitive to temperature and the degree of dewetting may be regarded as a crucial factor affecting the bonding between the particles. Considering the average thickness (approximately 17.5 nm) of the Ag shell, the size of most of the initial Ag bumps would be less than 20 nm. Because of the Gibbs–Thomson effect, however, the melting point of a Ag bump of this size would be significantly less,[22, 23] and thus coalescence between the Ag bumps by rapid solid-state sintering can be achieved quickly, resulting in bonding between the particles and the larger Ag bumps.

When the particles were heated to 250 °C, a greater change in the microstructure was observed. Specifically, the Ag phase was seen to penetrate the Cu core, which

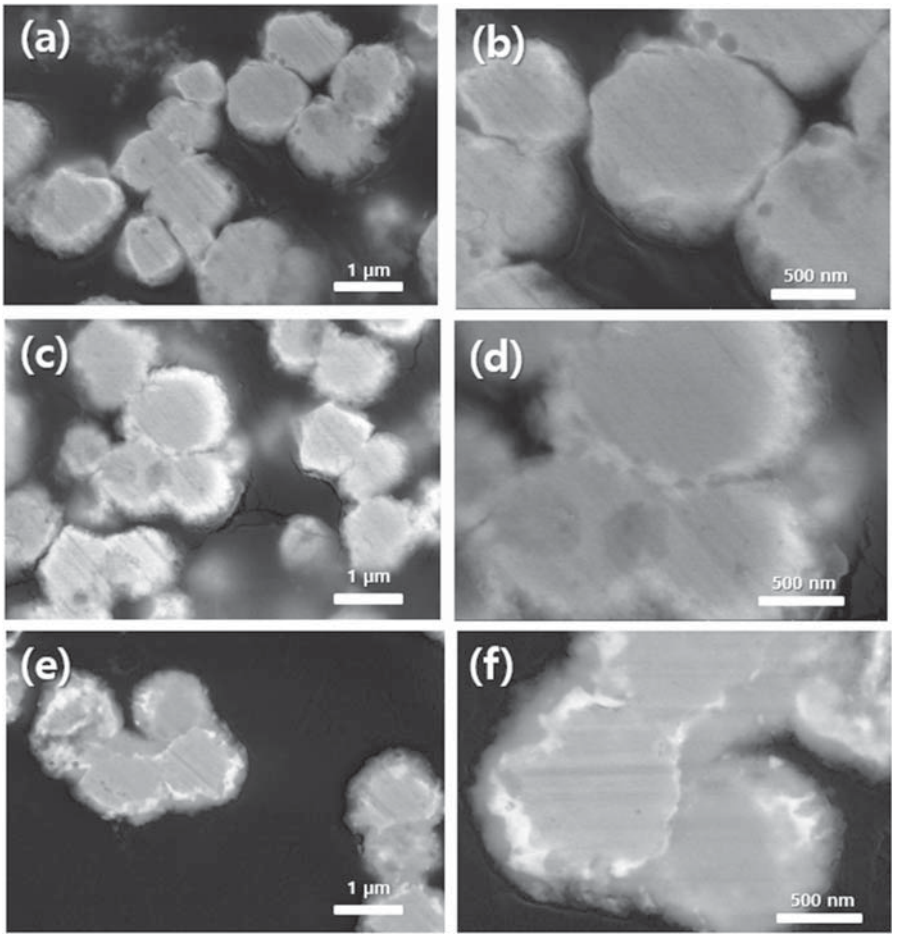

Fig. 2. Cross-sectional BSE images of Ag-coated Cu particles heat treated for 20 min at different temperatures: (a, b) 200 °C, (c, d), 225 °C, and (e, f) 250 °C.

was preceded by pronounced aggregation between the Ag-coated Cu particles. Hence, the bonding between the particles was strengthened at the interface, leading to a greater density. Moreover, the Ag phase was not detected at the neck formed between the particles. The neck interface between the particles that was formed to reduce the surface energy is a grain boundary diffusion site. Therefore, the Ag phase in the neck interface can be transported to the end points of the interface and eliminated from the initial position. The penetration of the Ag phase is assumed to be a result of the out-diffusion of the Cu core. In a Ag-coated Cu structure, the interior Cu atoms can out-diffuse abruptly through the thin Ag layer and then oxidize at 250 °C when a locally thin structure is formed in the Ag shell.[20] The main transport channel for the Cu diffusion would be grain boundaries in the thin Ag layer.[20]

The XRD results for Ag-coated Cu particles heated for 20 min at 200 °C, 225 °C, and 250 °C are shown in Figure 3. For the particles heated to 200 °C, no copper oxide phase was detected. However, traces of copper oxide were detected after heating to 225 °C, and the oxide phase (Cu_2O) was clearly visible after heating to 250 °C. These results are in good agreement with the oxidation mechanism of Cu discussed in reference to Figure 2.

Although the formation of Ag bumps did not destroy the coverage of the Ag shell, the very thin Ag layers locally created by the bump formation are assumed to be the main sites for the oxidation of the core Cu because the Cu atoms can spill out through the thin Ag layers.

By evaluating the thermal properties of the Ag-coated Cu particles, the microstructure of the bondline was elucidated after die bonding using the Ag-coated Cu particles. SEM images of the cross-sectionally fractured bondline heated for 20 min at 250 °C are shown in Figure 4. The thickness of bondline was 80 μm. In addition to the slight bonding between the Ag-coated Cu particles shown in Figure 4(a), the bonding between the Ag-coated Cu particles and Ag finish on the substrate is clearly observed in Figure 4(b).

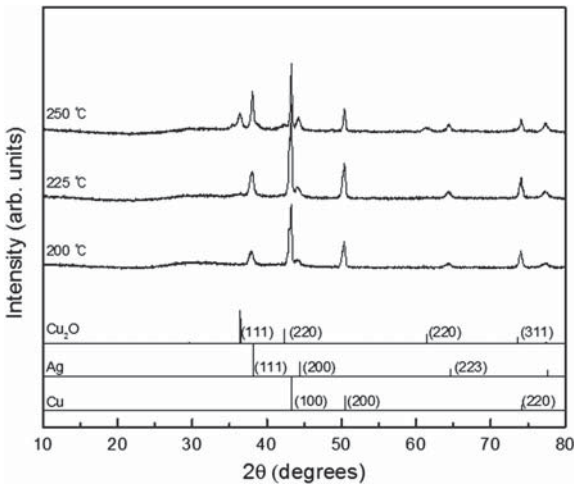

Fig. 3. XRD results of Ag-coated Cu particles heat treated for 20 min at different temperatures.

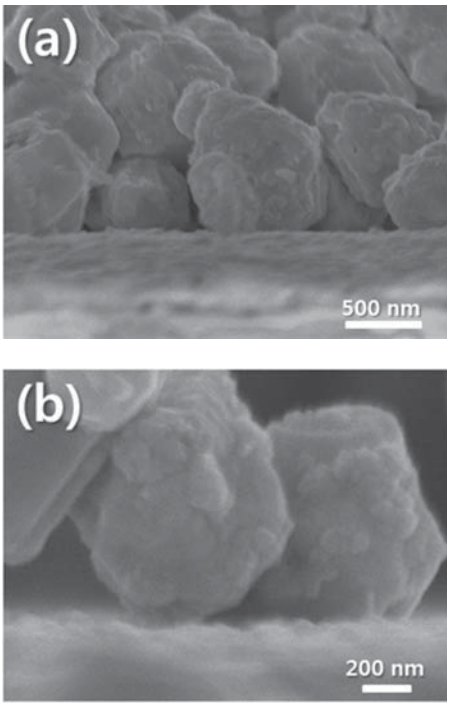

Fig. 4. (a) Low- and (b) high-magnification SEM images of cross-sectionally fractured bondline heat treated for 20 min at 250 °C.

Cross-sectional SEM images of the bondline heated for 20 min at 250 °C are shown in Figure 5. Although the density of the Ag-coated Cu particles was not very high, sufficient bonding between some of the particles is shown in Figures 5(a) and (b); it was also found that there was considerable bonding between the Ag-coated Cu particles and the Ag finish on the substrate, as shown in Figure 5(c). Meanwhile, voids were observed in the interior of some particles, as shown in Figure 5(a), with these forming after the above mentioned Cu out-diffusion.[20] These results clearly indicate the feasibility of die bonding at 250 °C using submicrometer Ag-coated Cu particles.

Figure 6 shows the shear strength of dies bonded to the Ag finish on the substrate using different bonding temperatures and times. For the die bonded at 200 °C, the shear strengths were very low in the case of bonding times of 5 or 10 min. The strength increased to 0.626 MPa as the bonding time increased to 20 min. The tendency for the bonding strength to increase with the bonding time was observed for all the bonding temperatures used in this study. For example, the bonding strength increased from 0.346 to 0.867 MPa at 225 °C and from 0.917 to 2.250 MPa at 250 °C. This means that a longer bonding time and a higher bonding temperature are crucial factors

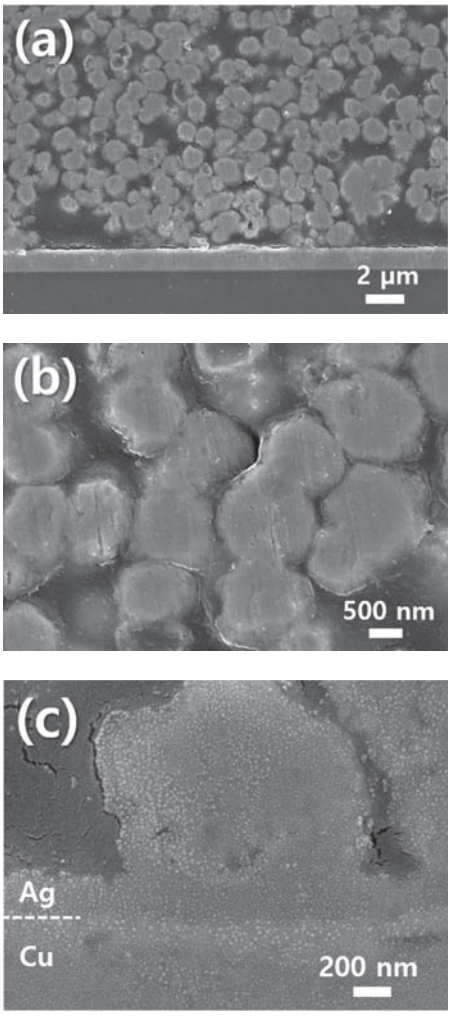

Fig. 5. Cross-sectional SEM images of bondline heat treated for 20 min at 250 °C: (a) low-magnification image, (b) sintered structure between Ag-coated Cu particles, and (c) bonding of Ag-coated Cu particles and Ag finish on substrate.

affecting the enhancement of the bonding strength owing to the increased solid-state Ag dewetting in the Ag-coated Cu particles. The relationship between the bonding time and the strength implies that the Ag dewetting behavior is a time-consuming process. Consequently, the adoption of a bonding temperature of 250 °C greatly increased the bonding strength. Furthermore, a bonding time of more than 10 min at this temperature greatly enhanced the strength, even without the application of bonding pressure during the die bonding with Ag-coated Cu particles.

Figure 7 shows SEM images of the fracture surface of the die after shear testing of a die bonded for 20 min at 250 °C. Most of the bondline, sintered with Ag-coated Cu particles, remained on the detached die, presenting a smooth fracture surface at low magnification (Fig. 7(a)). On the fracture surface observed at a high magnification

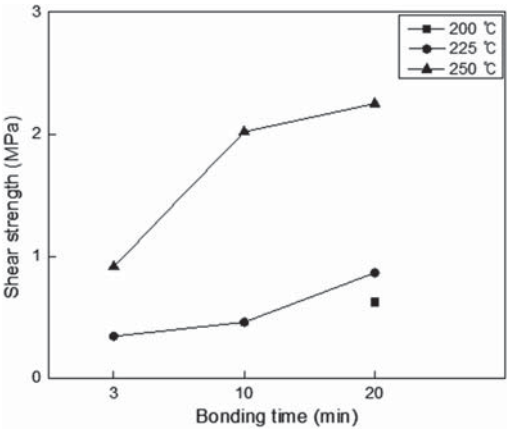

Fig. 6. Shear strength of dies bonded to Ag finish on substrate for different bonding temperatures and times.

(Fig. 7(b)), however, destruction of the sintered Ag-coated Cu particles occurred at slightly different heights, indicating the presence of a rough surface. Therefore, the main fracture site was judged to be the interface between the bondline structure and the Ag finish on the substrate, which resulted in only small amounts of Ag-coated Cu particles remaining on the Ag finish.

To enhance the bonding strength, resin infiltration and curing processes were added to the bondline formed for 20 min at 250 °C. Figure 8 shows cross-sectional SEM

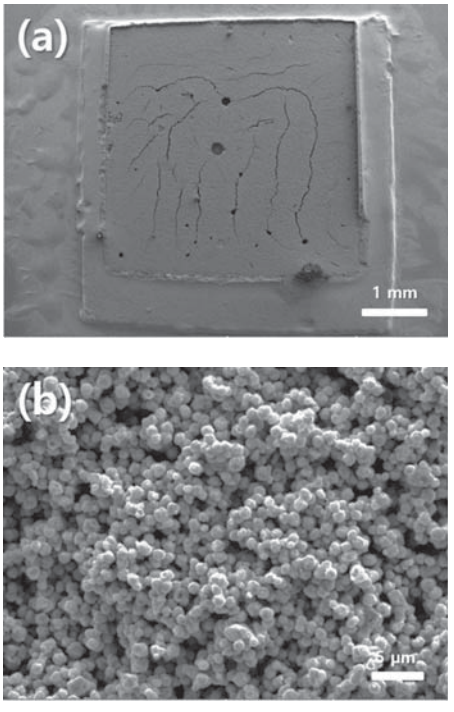

Fig. 7. (a) Low- and (b) high-magnification SEM images of fracture surface of a die after shear test with die bonded for 20 min at 250 °C.

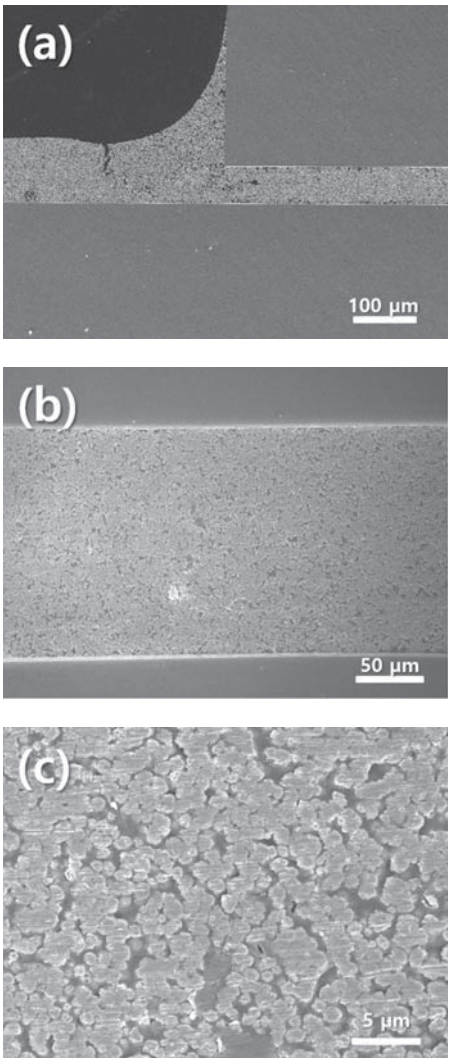

Fig. 8. Cross-sectional SEM images of bondline infiltrated with resin formulation after die bonding using Ag-coated Cu particles.

images of the bondline infiltrated and cured with a resin formulation after die bonding. A fillet was formed around the edge of the die (Fig. 8(a)). It was also found that the resin formulation completely penetrated across the bondline (Figs. 8(b and c)). The microstructure of the bondline was locally nonhomogeneous at high magnification (Fig. 8(c)) but homogeneous through the bondline at low magnification (Fig. 8(b)).

Figure 9 compares the displacement–force curves during the die shear test as a function of the resin infiltration/curing. Die bonding was conducted for 20 min at 250 °C. Immediately after die bonding using the Ag-coated Cu paste, the displacement–force curve was drawn as a short parabola, with a maximum shear strength of only 2.25 MPa, indicating a low fracture energy. However, the curve lengthened considerably and assumed a slightly

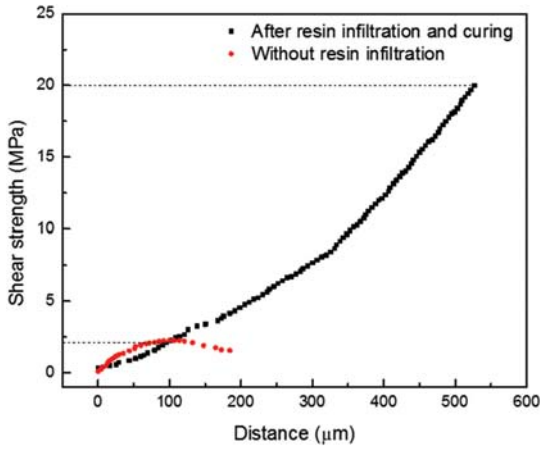

Fig. 9. Comparison of displacement–force curves for die shear test as function of resin infiltration.

linear shape with the addition of the resin infiltration and curing processes. The die fractured at 19.991 MPa during the shear test and the displacement also increased. This result confirms the enhanced fracture energy property at the bondline as a result of the infiltration and curing processes.

SEM images of the fracture surface on the substrate after the shear test using a die reinforced by resin

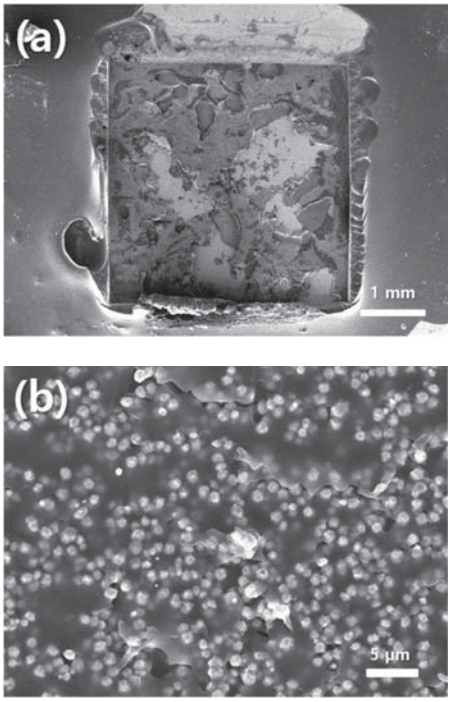

Fig. 10. (a) Low- and (b) high-magnification SEM images of fracture surface on substrate after shear test using a die reinforced by resin infiltration and curing.

infiltration and curing are shown in Figure 10. The die broke into fractions immediately after the shear test, indicating the greatly enhanced shear strength and fracture energy of the bondline. Although infiltration of the resin formulation was not observed in some locations on the fractured surface (Fig. 10(a)), the infiltration was sufficiently homogeneous with only a small proportion of voids at low magnifications, indicating the occurrence of wetting of the Ag-coated Cu particles and penetration between the Ag-coated Cu particles by capillary force. Because most of the bondline structure remained on the substrate, the fractured surface was judged to be the interface between the bondline and the die.

4. CONCLUSIONS

After heating the fabricated submicrometer Ag-coated Cu particles for 20 min, the formation of bumps on the surface and slight bonding between the particles were observed at 225 °C, whereas a rougher surface, strong bonding between the particles, and out-diffusion of Cu through the Ag layer were observed at 250 °C. The XRD results indicated that the outermost phase at 250 °C is copper oxide (Cu_2O). These results imply that the solid-state Ag dewetting behavior is sensitive to temperature, whereas the degree of dewetting is a crucial factor affecting the bonding between the particles. The bonding strength in a die bonded using Ag-coated Cu particles increased with increasing bonding temperature and time. The die bonded for 20 min at 250 °C had a bonding strength of 2.25 MPa. This increased to 19.991 MPa as a result of the enlarged displacement after resin infiltration and curing. These results demonstrate that die bonding using Ag-coated Cu particles is feasible even when no bonding pressure is applied during the bonding.

Acknowledgment: This work was supported by Nano-Convergence Foundation (www.nanotech2020.org) funded by the Ministry of Science, ICT and Future Planning (MSIP, Korea) and the Ministry of Trade, Industry and Energy (MOTIE, Korea) [Project Name: Commercialization of 100 Gbps optical receiver and transmitter modules based on nano Ag-coated Cu paste].

References and Notes

1. X. Xu, X. Luo, and H. Zhang, *Mater. Lett.* 57, 3987 (**2003**).
2. H. T. Hai, J. G. Ahn, D. J. Kim, J. R. Lee, H. S. Chung, and C. O. Kim, *Surf. Coat. Technol.* 201, 3788 (**2006**).
3. M. Grouchko, A. Kamyshny, and S. Magdassi, *J. Mater. Chem.* 117, 3057 (**2009**).
4. R. Zhang, W. Lin, K. Lawrence, and C. P. Wong, *Int. J. Adhe. Adhes.* 30, 403 (**2010**).
5. J. Zhao, D. M. Zhang, and J. Zhao, *J. Solid State Chem.* 184, 2339 (**2011**).
6. D. S. Jung, H. M. Lee, Y. C. Kang, and S. B. Park, *J. Colloid Interface Sci.* 364, 574 (**2011**).
7. Y. Peng, C. Yang, K. Chen, S. R. Popuri, C.-H. Lee, and B.-S. Tang, *Appl. Surf. Sci.* 263, 38 (**2012**).
8. A. Muzikansky, P. Nanikashvili, J. Grinblat, and D. Zitoun, *J. Phys. Chem. C* 117, 3093 (**2013**).
9. H. T. Hai, H. Takamura, and J. Koike, *J. Alloys Compd.* 564, 71 (**2013**).
10. G. Kim, K.-M. Jung, J.-T. Moon, and J.-H. Lee, *J. Microelectron. Packag. Soc.* 21, 51 (**2014**).
11. H.-W. Cui, J.-T. Jiu, T. Sugahara, S. Nagao, K. Suganuma, and H. Uchida, *Electron. Mater. Lett.* 11, 315 (**2015**).
12. E. B. Choi and J.-H. Lee, *J. Alloys Compd.* 643, S231 (**2015**).
13. E. B. Choi and J.-H. Lee, *J. Alloys Compd.* 689, 952 (**2016**).
14. C.-H. Tsai, S.-Y. Chen, J.-M. Song, I.-G. Chen, and H.-Y. Lee, *Corros. Sci.* 74, 123 (**2013**).
15. S.-S. Chee and J.-H. Lee, *J. Mater. Chem. C* 2, 5372 (**2014**).
16. Y. M. Shin, J. H. Kim, and J.-H. Lee, *J. Nanosci. Nanotechnol.* 16, 11523 (**2016**).
17. J. Hwang, M. Park, S. Jang, H. Choi, J. Jang, Y. Yoo, H. Jo, and M. Jeon, *J. Nanosci. Nanotechnol.* 17, 3487 (**2017**).
18. H. B. Lee and J.-H. Lee, *Nanosci. Nanotechnol. Lett.* 8, 100 (**2016**).
19. H.-C. Bae, Y.-S. Eom, K.-S. Choi, S.-E. Moon, and J.-H. Lee, *J. Nanosci. Nanotechnol.* 16, 12732 (**2016**).
20. J. H. Kim and J.-H. Lee, *Jpn. J. Appl. Phys.* 55, 06JG01-1 (**2016**).
21. S. W. Park, T. Sugahara, M. Haramura, N. Kagami, S. Sakamoto, and K. Suganuma, *Mater. Lett.* 151, 68 (**2015**).
22. Y. F. Zhu, J. S. Lian, and Q. Jiang, *J. Phys. Chem. C* 113, 16896 (**2009**).
23. T. Yonezawa, S. Arai, H. Takeuchi, T. Kamino, and K. Kuroda, *Chem. Phys. Lett.* 537, 65 (**2012**).

Received: 20 January 2017. Accepted: 2 May 2017.